GSA DATA REPOSITORY 2010230

(U-Th)/He thermochronometry constraints on unroofing of the eastern Kaapvaal craton and significance for uplift of the southern African Plateau

Rebecca M. Flowers, Blair Schoene

DATA REPOSITORY

(U-Th)/He Analytical Methods

Individual fragments of titanite and single crystals of apatite were selected based on morphology and clarity. Mineral inclusions in apatite crystals were avoided using a binocular microscope with crossed polars. Prior to analysis, grains were photographed and dimensions measured.

Most apatite grains were packaged in Pt packets and laser heated to 1065 _C for eight minutes (House et al., 2000). Extracted He gas was spiked with ^{3}He, purified using cryogenic and gettering methods, and analyzed on a quadrupole mass spectrometer. The degassed apatites were retrieved, spiked with a ^{235}U-^{230}Th-^{145}Nd-^{51}V tracer, dissolved in HNO_3 at ~90 _C for 1 hour, and analyzed on an Agilent ICP-MS at the California Institute of Technology. The apatite mass was computed from the apatite Ca concentration using ^{51}V as an elemental spike. This Ca-based mass was used to calculate the apatite U and Th concentrations. Fragments of the Durango apatite standard were analyzed by the same procedures with the batch of unknowns. A hexagonal prism morphology was used for the alpha-ejection correction (Farley et al., 1996).

Single titanite fragments and two individual apatite crystals (from sample KPV99-91) were loaded into sapphire microfurnaces and laser heated to 1300 _C for eight minutes at the

California Institute of Technology. Extracted He gas was spiked with ^{3}He, purified using cryogenic and gettering methods, and analyzed on a quadrupole mass spectrometer. The degassed grains were then retrieved. At the University of Colorado, Boulder, the grains were loaded into Teflon capsules, spiked with a mixed ^{235}U-^{230}Th tracer, and dissolved in 29 M HF at 200 _C for ~100 hours followed by conversion to 6 M HCl at 180 _C for 12 hours. Samples were dried down, taken up in dilute HNO_3, and analyzed on the Element 2 ICP-MS at the University of Colorado, Boulder. Grain masses were determined using the measured dimensions of the crystal. Fragments of Bolivian titanite and zircon of known age (Farley et al., 2006) were used as standards and analyzed by the same procedure with the batch of unknowns. A hexagonal prism morphology and the alpha-ejection correction of Farley et al. (1996) was applied to the two apatite crystals analyzed by this method. No alpha-ejection correction was applied to the titanites because they were fragments of larger grains. Some scatter in the results may be attributable to uncertainties in this correction if the analyzed fragments contained portions of grain edges and thus lost some fraction of their He due to ejection. Previous evaluation of this source of error suggested that the fraction of He lost by alpha-ejection is likely to be <10% for fragments derived from titanites of typical grain size (Reiners and Farley, 1999). Reiners and Farley (1999) found that radiation damage for titanites of 50-300 ppm U and Th concentration and 150 Ma of damage accumulation did not have a significant effect on titanite He diffusion. Despite the older (U-Th)/He dates for the Kaapvaal titanites, their low U and Th values means that they are almost certainly characterized by less radiation damage than the titanites studied by Reiners and Farley (1999). The analyzed Kaapvaal titanites were characterized by mean U and Th values of 7.4 ppm and 0.7 ppm respectively. Titanites from AGC01-4 previously analyzed by U-Pb TIMS were characterized by 4-50 ppm U (Schoene and

Bowring, 2007). Thus, radiation damage-facilitated He loss should not be a significant factor influencing our titanite results.

REFERENCES

Farley, K.A. Wolf, R.A., and Silver, L.T., 1996, The effects of long alpha-stopping distances on (U-Th)/He ages: Geochimica et Cosmochimica Acta, v. 60, p. 4223-4229.

Farley, K.A., Libarkin, J., Mukhopadhyay, S., and Amidon, W., 2006, Cosmogenic and nucleogenic ^{3}He in apatite, titanite and zircon: Earth and Planetary Science Letters, v. 248, p. 451-461.

House, M.A., Farley, K.A., and Stockli, D., 2000, Helium chronometry of apatite and titanite using Nd-YAG laser heating: Earth and Planetary Science Letters, v. 183, p. 365-368.

Reiners, P.W., and Farley, K.A., 1999, Helium diffusion and (U-Th)/He thermochronometry of titanite: Geochimica et Cosmochimica Acta, v. 63, p. 3845-3859.

Schoene, B. and Bowring, S.A., 2007, Determining accurate temperature-time paths from U-Pb thermochronology: An example from the Kaapvaal craton, southern Africa: Geochimica et Cosmochimica Act, v. 71, p. 165-185.

FIGURE CAPTIONS

Figure DR1. (A) Elevation vs. mean apatite (U-Th)/He date. (B) Mean apatite (U-Th)/He date versus mean apatite eU, with uncertainties plotted as the sample standard deviation. The two samples with only two analyses are excluded from both plots.

Figure DR2. Thermal histories predicted by the inverse modeling simulations for the four coastal plain samples with ca. 100 Ma dates. The constraints imposed on the thermal history are described in the main text and shown by the black squares and gray rectangles. The results are depicted as fields encompassing the thermal histories over the full 1.2 Ga duration of the simulations. The dark and light grays represent good and acceptable fits, respectively. The bold black line depicts the “best-fit” thermal history.

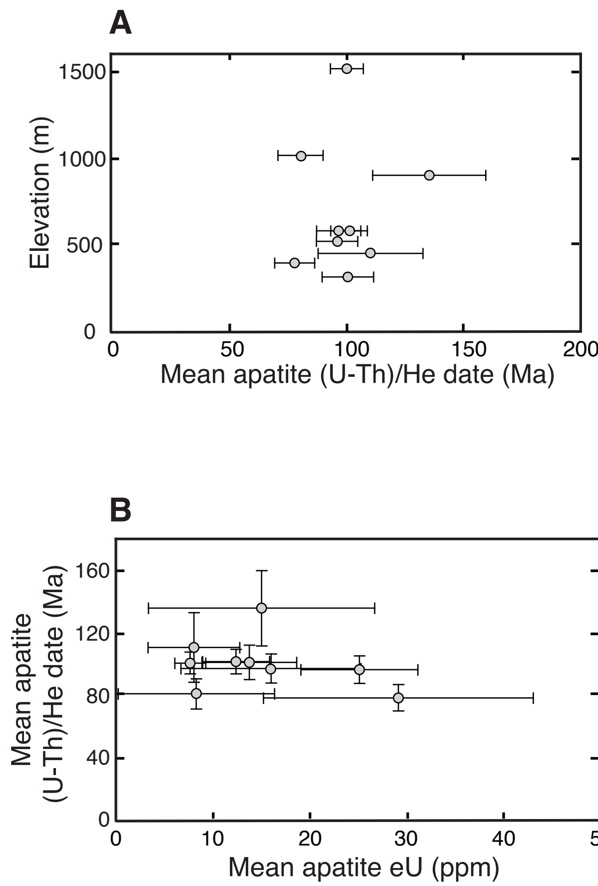

Flowers and Schoene
Figure DR1

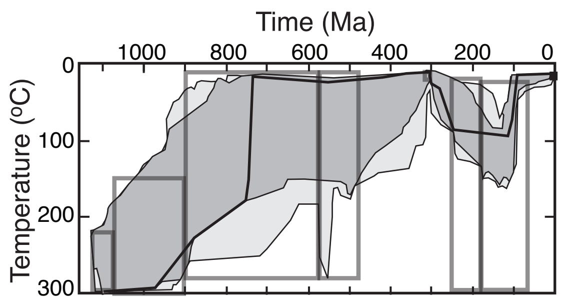

Flowers and Schoene
Figure DR2

Table DR1. Apatite and titanite (U-Th)/He data

Sample	Mass (ug)	Radius (um)	Length (um)	Ft[a]	U (ppm)	Th (ppm)	Sm (ppm)	He (nmol/g)	Effective U (ppm)	Raw date (Ma)	Corr date (Ma)	Est 1σ[b] err (Ma)
Apatite												
KPV99-94: Nelshootge pluton, foliated granodiorite; 25.8912 S, 30.6235 E, 1015 m												
a2	2.3	89	145	0.71	4.2	3.9	34.4	1.6	5.1	57	**80**	3
a3	1.7	81	130	0.69	20.3	0.5	30.2	7.0	20.4	63	**92**	3
a4	1.6	79	127	0.67	3.3	4.0	26.1	1.1	4.2	46	**68**	3
a5	1.7	80	132	0.68	3.5	0.6	16.6	1.1	3.6	56	**82**	4
KPV99-91: Stentor pluton, late pegmatite dike; 25.6497 S, 31.2426, 500 m												
a1	11.0	84	194	0.81	12.1	2.8	NA	5.4	12.8	77	**94**	4
a3	9.6	81	185	0.81	5.5	2.1	NA	2.8	6.0	85	**106**	6
KPV99-96: Stolzberg pluton, tonalite gneiss; 26.0218 S, 30.7442 E, 955 m												
a1	2.3	79	180	0.68	3.2	1.5	118.2	1.8	3.6	89	**131**	6
a4	0.9	65	107	0.58	1.4	4.4	114.3	1.0	2.4	72	**122**	7
EKC02-40:Steynsdorp pluton, foliated tonalite-granodiorite; 26.1779 S, 30.9604 E, 1515 m												
a1	4.7	57	177	0.75	6.1	0.7	60.2	2.4	6.3	69	**91**	3
a2	3.9	49	205	0.72	9.5	3.3	93.2	4.6	10.3	81	**111**	3
a3	2.4	44	150	0.69	6.8	4.0	58.4	2.9	7.8	68	**99**	3
a4	2.2	45	136	0.68	7.0	1.9	60.8	2.9	7.4	71	**103**	4
a5	2.2	43	147	0.68	6.1	2.0	65.9	2.5	6.6	68	**99**	3
AGC01-4: Usutu suite, foliated tonalite; 25.8952 S, 31.3069 E, 580 m												
a1	1.4	36	138	0.63	7.6	4.3	61.4	2.8	8.7	59	**93**	3
a2	1.5	36	140	0.63	11.9	4.0	85.2	4.2	12.9	59	**93**	3
a3	3.2	46	185	0.71	8.7	2.3	125.4	4.0	9.3	77	**107**	3
a4	1.3	34	141	0.62	13.4	3.9	53.6	5.1	14.4	64	**103**	4
a5	3.9	50	195	0.73	15.6	4.7	81.8	7.4	16.8	80	**110**	3
AGC01-5: Ancient Gneiss Complex, tonalite gneiss; 25.8961 S, 31.3104 E, 580 m												
a1	4.0	47	219	0.72	9.2	3.7	27.2	4.2	10.1	76	**105**	3
a2	3.3	51	159	0.72	18.4	6.1	52.4	6.7	20.0	61	**84**	3
a3	1.9	37	169	0.65	11.4	3.7	38.7	4.1	12.3	61	**92**	3
a4	3.9	49	202	0.73	28.4	7.8	82.2	13.0	30.3	78	**108**	3
a5	1.6	37	143	0.64	6.8	2.4	23.7	2.5	7.4	62	**96**	3
AGC01-2: Ancient Gneiss Complex, tonalite gneiss; 26.7141 S, 31.0448 E, 900 m												
a1	2.5	101	119	0.70	26.2	10.0	87.7	11.9	28.5	76	**108**	3
a2	2.6	91	153	0.70	8.1	0.6	142.1	5.0	8.2	108	**154**	5
a4	1.8	78	147	0.67	8.1	1.2	248.0	4.6	8.4	97	**145**	6
BS04-7: Usutu Suite, Tsawela gneiss, tonalite gneiss; 26.5766 S, 31.3455 E, 450 m												
a1	7.9	120	270	0.78	5.1	1.4	252.7	2.5	5.5	80	**102**	3
a2	3.8	91	223	0.70	7.6	30.9	290.7	7.4	14.9	88	**125**	4
a4	2.1	85	144	0.69	5.2	10.0	236.6	3.9	7.5	92	**132**	5
a5	2.0	83	142	0.68	4.4	0.2	231.7	1.5	4.4	57	**83**	4
EKC02-64: Nhlangano gneiss; 26.6675 S, 31.3977 E, 315 m												
a1	3.3	102	156	0.72	18.1	5.5	214.3	8.2	19.4	77	**105**	3
a3	1.9	86	128	0.68	9.9	2.0	149.1	4.3	10.4	74	**109**	4
a4	4.0	138	105	0.78	11.6	0.0	156.5	4.4	11.6	69	**88**	2
EKC03-35: Nhlangano gneiss; 26.8760 S, 31.2805 E, 385 m												
a1	1.9	88	120	0.67	35.9	32.7	157.3	13.5	43.6	57	**84**	2
a2	1.4	74	126	0.64	31.9	6.8	276.3	8.0	33.5	43	**68**	2
a3	1.5	79	120	0.65	9.8	2.2	219.0	2.8	10.3	49	**75**	3
a4	0.9	70	93	0.60	25.9	14.6	357.0	8.4	29.3	52	**86**	3
EKC02-65: Hlatikulu granite; 26.7349 S, 31.4008 E, 520 m												
a1	1.8	80	140	0.65	15.4	39.8	162.5	8.3	24.7	61	**93**	3
a2	1.4	69	143	0.63	18.7	65.7	257.9	12.1	34.2	64	**102**	3
a3	1.2	72	112	0.63	11.2	39.3	168.4	7.7	20.4	68	**108**	4
a4	1.0	64	116	0.58	11.2	33.7	151.6	5.2	19.1	50	**86**	4
a5	4.5	130	132	0.77	16.9	44.3	168.2	10.7	27.3	71	**92**	2
Titanite												
EKC02-40: Steynsdorp pluton, foliated tonalite-granodiorite; 26.1779 S, 30.9604 E, 1515 m												
t2	33.2	99	242	1	4.1	0.1	NA	21.8	4.2	871	**871**	36
t4	23.9	85	239	1	16.7	0.3	NA	67.8	16.7	689	**689**	21
AGC01-4: Usutu suite, foliated tonalite; 25.8952 S, 31.3069 E, 580 m												
t3	13.9	71	196	1	4.4	0.7	NA	16.9	4.6	636	**636**	26
t5	21.5	82	230	1	4.3	1.8	NA	20.1	4.7	725	**725**	25

[a]Ft is alpha ejection correction of Farley et al., 1996; [b] 1-sigma errors propagated from U, Th and He measurement uncertainties and grain-length measurement uncertainty